

Form-finding of a tensegrity structure as an optimisation problem

Tiago Pereira, Casper Lindeman, Gonchigsuren Bor, Rasmus Grødeland

June 3, 2024

Abstract

Using theory from the field of optimisation, we prove that it is possible to determine valid shapes of a variety of different tensegrity structures, including cable-nets, tensegrity domes and freestanding structures, through the minimisation of the structures' energy function. We model the energy as a function of the forces acting on it, where some structural joints have been fixed, and in cases where the structure is entirely above ground. Using the BFGS method with weak Wolfe conditions, possible shapes are computed for each of the above mentioned structures, where a quadratic penalty term is added to account for the ground profile in cases where the structure is freestanding.

Introduction

In this report, we discuss the optimisation problem of *form-finding* with respect to *tensegrity structures*. Tensegrity structures are mechanical structures consisting of bars and elastic cables that are connected at joints, referred to as nodes in the scope of this report. Together, the bars and cables guarantee the stability of the structure, whose integrity is a result of tension in the structural members and compression of the structure's bars.

We model the tensegrity structure as a directed graph $\mathcal{G} = (\mathcal{V}, \varepsilon)$, with vertex set $\mathcal{V} = \{1, \dots, N\}$ and edge set $\varepsilon \subset \mathcal{V} \times \mathcal{V}$. The vertices represent the nodes in the structure, and an edge $e_{ij} = (i, j)$ with $i < j$ indicates that the nodes i, j are connected through either a bar or a cable. We furthermore denote by $x^{(i)} = (x_1^{(i)}, x_2^{(i)}, x_3^{(i)}) \in \mathbb{R}^3$, the position of node i relative to the other nodes in the structure. Consequently, the position of all nodes is given by $X = (x^{(1)}, \dots, x^{(N)}) \in \mathbb{R}^{3N}$, which we will refer to as a structure in the subsequent sections. The energy of any given structure is then found by solving

$$E(X) = \sum_{e_{ij} \in \mathcal{B}} (E_{\text{elast}}^{\text{bar}}(e_{ij}) + E_{\text{grav}}^{\text{bar}}(e_{ij})) + \sum_{e_{ij} \in \mathcal{C}} E_{\text{elast}}^{\text{cable}}(e_{ij}) + E_{\text{ext}}(X), \quad (1)$$

where $\mathcal{B}, \mathcal{C} \subset \mathcal{E}$ denote the set of bars and cables in the structure, respectively. The total energy $E(X)$ given in (1), consists of elastic energy from the structure's bars $E_{\text{elast}}^{\text{bar}}$, elastic energy from the structure's cables $E_{\text{elast}}^{\text{cable}}$, gravitational energy $E_{\text{grav}}^{\text{bar}}$, as a result of the mass of the structural bars, and energy contributed by external loads E_{ext} . We define these contributions as follows,

$$E_{\text{elast}}^{\text{bar}}(e_{ij}) = \frac{c}{2\ell_{ij}^2} (L(e_{ij}) - \ell_{ij})^2 = \frac{c}{2\ell_{ij}^2} (\|x^{(i)} - x^{(j)}\| - \ell_{ij})^2, \quad (2)$$

$$E_{\text{elast}}^{\text{cable}}(e_{ij}) = \begin{cases} \frac{k}{2\ell_{ij}^2} (L(e_{ij}) - \ell_{ij})^2 = \frac{k}{2\ell_{ij}^2} (\|x^{(i)} - x^{(j)}\| - \ell_{ij})^2 & \text{if } L(e_{ij}) > \ell_{ij}, \\ 0 & \text{if } L(e_{ij}) \leq \ell_{ij}, \end{cases} \quad (3)$$

$$E_{\text{grav}}^{\text{bar}}(e_{ij}) = \frac{\rho g \ell_{ij}}{2} (x_3^{(i)} + x_3^{(j)}) \quad (4)$$

$$E_{\text{ext}}(X) = \sum_{i=1}^N m_i g x_3^{(i)}, \quad (5)$$

where we assume that $\rho g, m_i, k, c > 0$ and that $L(e_{ij})$ indicates the *resting length* of e_{ij} . Furthermore, we introduce two constraints, constraints one and two, given by

$$x^{(i)} = p^{(i)} \quad \text{for } i = 1, \dots, M, \quad (6)$$

and

$$x_3^{(i)} \geq f(x_1^{(i)}, x_2^{(i)}) \quad \text{for all } i = 1, \dots, N, \quad (7)$$

General analysis of the energy function given both constraints

Consider the problem of minimising the total energy given by (1) with constraints given by (6), that is, the constraint of fixing some of the nodes of the structure.

Theorem 1 *Minimising the total energy function given by (1) with constraint (6) admits a solution provided that the graph \mathcal{G} is connected and $k, c > 0$.*

We want to show that the minimisation problem admits a solution, i.e. has a global minimum, provided that \mathcal{G} is connected. To do so, we must show that (1) is lower semi-continuous, coercive and that \mathcal{G} has to be connected.

Lower semi-continuity: To show that $E(X)$ is lower semi-continuous (LSC), recall that every continuous function $f : \mathbb{R}^d \rightarrow \mathbb{R}$ is also lower semi-continuous. We thus want to show that (1) is continuous for all $x \in \mathbb{R}^d$. Showing that (1) is continuous is relatively straightforward, and all we have to do is to show that its components, that is, $E_{\text{bar}}^{\text{elast}}, E_{\text{bar}}^{\text{grav}}, E_{\text{cable}}^{\text{elast}}$ and E_{ext} are continuous. As one can see, all terms in $E(X)$ are either polynomials or norms. Since both polynomials and norms are continuous, the equation for total energy has to be continuous as well. Moreover, the equation for the total energy remains continuous even with constraint (6), as we merely change the nodes $x^{(i)}$ with constant nodes $p^{(i)}$ such that the function remains a function of polynomials and norms. Thus, $E(X)$ is LSC even with the first constraint. Now that we have shown that E is continuous, and hence LSC, it remains to show that E is coercive as well.

Coercivity: To show that E subject to the constraint given by (6) is coercive, recall that $c, k, \rho g$ and m_i are non-negative constants, assume that we can stretch the bars and cables in the structure as much as we want, and let $p^{(j)} \in \mathbb{R}^3$, where $1 \leq j \leq M$ be a fixed node. Moreover, assume that the graph \mathcal{G} is connected such that there exists a path from $x^{(i)}$ to $p^{(j)}$ connected through bars and cables, and recall that a function $f : \mathbb{R}^d \rightarrow \mathbb{R}$ is coercive if, for all sequences $\{x_k\}_{k \in \mathbb{N}}$, where $\|x_k\| \rightarrow \infty$ as $k \rightarrow \infty$,

$$\lim_{k \rightarrow \infty} f(x_k) = +\infty.$$

Since in our case X is a vector containing all nodes in the structure, then, whenever $\|X\| \rightarrow \infty$, at least one of the nodes in the structure needs to go to infinity such that $\|x^{(i)}\| \rightarrow \infty$. In such case, $\|x^{(i)} - p^{(j)}\| \rightarrow \infty$. Note that a case where $p^{(j)}$ is located infinitely far away from the origin is not possible as $p^{(j)} \in \mathbb{R}^3$. Then, due to the assumptions above, at least one of the cables or bars will be stretched to infinity. This implies that $E_{\text{bar}}^{\text{elast}} \rightarrow +\infty$ or $E_{\text{cable}}^{\text{elast}} \rightarrow +\infty$, for all sequences $\{X_k\}_{k \in \mathbb{N}}$ such that $\|X_k\| \rightarrow \infty$ as $k \rightarrow \infty$. Given that $\rho g, m_i > 0$, the only terms in E that can become negative are the linear terms $E_{\text{grav}}^{\text{bar}}$ and E_{ext} . However, the quadratic terms $E_{\text{bar}}^{\text{elast}}$ and $E_{\text{cable}}^{\text{elast}}$ in E will grow faster than the linear terms such that

$$\lim_{k \rightarrow \infty} E(X_k) = +\infty, \quad \forall \{X_k\}_{k \in \mathbb{N}} \text{ s.t. } \lim_{k \rightarrow \infty} \|X_k\| = \infty.$$

Thus, E subject to the constraint in (6) is coercive, provided that \mathcal{G} is connected and that $c, k > 0$.

The reason we need the graph \mathcal{G} to be connected or that $c, k > 0$ is that if \mathcal{G} were not connected, then $\|x^{(i)} - p^{(j)}\| \rightarrow \infty$ would not imply that $E_{\text{bar}}^{\text{elast}} \rightarrow +\infty$ or $E_{\text{cable}}^{\text{elast}} \rightarrow +\infty$. Therefore,

$$\lim_{k \rightarrow \infty} E(X_k) = +\infty$$

is not necessarily true, and E is not coercive. Thus, minimising E with constraint (6) admits a solution provided that the graph \mathcal{G} is connected and that $c, k > 0$.

Moving on further, we now want to analyse the behaviour of the energy function with a new constraint (7).

Theorem 2 *Minimising (1) with constraint (7) admits a solution if $f \in C^1(\mathbb{R}^2)$ is coercive and $m, \rho g > 0$.*

To prove our theorem, we need to show that (1) is lower semi-continuous and coercive subject to constraint (7).

Lower semi-continuity: As shown in theorem 1, our energy function E consists of polynomial terms and norms which are continuous by definition. Furthermore, the second constraint (7) is a continuous constraint since $f \in C^1(\mathbb{R}^2)$. Thus, E remains a continuous function under the second constraint, and since continuous functions are LSC, E is LSC with the second constraint.

It remains now to show that E is coercive if $f \in C^1(\mathbb{R}^2)$ is coercive.

Coercivity: Consider at first a structure without any mass. Shifting the structure upwards only, the gravitational energy does not change, meaning that E remains constant and is not coercive. We therefore need $m, \rho g > 0$ for E to be coercive. By constraint (7) and $f \in C^1(\mathbb{R}^2)$ being coercive, we get

$$x_3^{(i)} \geq f(x_1^{(i)}, x_2^{(i)}) > -\infty. \quad (8)$$

Furthermore, recall that the only terms in E that can be negative are $E_{\text{grav}}^{\text{bar}}$ and E_{ext} . As $E_{\text{grav}}^{\text{bar}}$ and E_{ext} are directly proportional to $x_3^{(i)}$, by (8) both $E_{\text{grav}}^{\text{bar}}$ and E_{ext} have to be bounded from below and hence, $E_{\text{grav}}^{\text{bar}}, E_{\text{ext}} > -\infty$. Thus, E is bounded from below.

Now that we have shown that E is bounded from below, we want to show that whenever $\|X\| \rightarrow \infty$, then $E_{\text{ext}} \rightarrow \infty$ such that $E(X) \rightarrow \infty$ and is thus coercive. To do so, recall that $\|X\| \rightarrow \infty$ implies that there exists at least one node $x^{(i)}$ such that $\|x^{(i)}\| \rightarrow \infty$.

Consider the case where $\|(x_1^{(i)}, x_2^{(i)})\| \rightarrow \infty$. Then, by coercivity,

$$\lim_{\|(x_1^{(i)}, x_2^{(i)})\| \rightarrow \infty} f(x_1^{(i)}, x_2^{(i)}) = \infty.$$

Since the lower bound for $x_3^{(i)}$ is $f(x_1^{(i)}, x_2^{(i)})$, the equation above implies that $x_3^{(i)} \rightarrow \infty$ as $\|(x_1^{(i)}, x_2^{(i)})\| \rightarrow \infty$. Conversely, whenever $\|(x_1^{(i)}, x_2^{(i)})\| \not\rightarrow \infty$ but $\|x^{(i)}\| \rightarrow \infty$ still holds, then $|x_3^{(i)}| \rightarrow \infty$. Thus, together with our findings in (8), $x_3^{(i)} \rightarrow \infty$. This means that whenever $\|x^{(i)}\| \rightarrow \infty$, $x_3^{(i)} \rightarrow \infty$. Hence, $E_{\text{ext}} \rightarrow \infty$ as $\|x^{(i)}\| \rightarrow \infty$, which in turn means that

$$\lim_{\|X\| \rightarrow \infty} E(X) = \infty,$$

and thus, E is coercive provided that $f \in C^1(\mathbb{R}^2)$ is coercive. Since E is LSC and coercive, provided that $f \in C^1(\mathbb{R}^2)$ is coercive then, minimising (1) admits a solution.

Furthermore, with a flat-ground constraint, i.e.

$$x_3^{(i)} \geq f(x_1^{(i)}, x_2^{(i)}) = 0 \quad \forall x_1^{(i)}, x_2^{(i)} \in \mathbb{R},$$

E will not be coercive anymore. This is due to the fact that we could simply shift the structure horizontally along the ground so that $\|X\|$ increases without ever increasing the total energy. However, since the terms E_{ext} and $E_{\text{grav}}^{\text{bar}}$ are bounded from below by the flat-ground constraint, we cannot eliminate the possibility of E having a global minimiser. If such a minimiser exists, it will not be unique as it will still be possible to shift the structure along the xy -plane. As a matter of fact, there would be infinitely many solutions.

Cable-nets

Consider the case where all the structural members are cables, and where we impose the additional constraints in (6). Possible shapes of the resulting *cable net* X^* , can then be determined by minimising

$$E(X) = \sum_{e_{ij} \in \mathcal{C}} E_{\text{elast}}^{\text{cable}}(e_{ij}) + E_{\text{ext}}(X), \quad \text{s.t. } x^{(i)} = p^{(i)}, \quad i = 1, \dots, M. \quad (9)$$

Theorem 3 *The function given by (9) is C^1 but typically not C^2 .*

We want to show that the function above is continuously differentiable, and so we examine its gradient ∇E . We start by defining the gradient operator with respect to node $i \in \mathcal{V}$, as $\nabla^{(i)} := (\partial_{x_1^{(i)}}, \partial_{x_2^{(i)}}, \partial_{x_3^{(i)}})^T$. Since the gradient is linear, we may express ∇E in terms of the gradient relative to each node, i.e.

$$\nabla E = \left(\nabla^{(M+1)} E, \dots, \nabla^{(N)} E \right)^T \in \mathbb{R}^{3(N-M)}, \quad (10)$$

where

$$\nabla^{(i)} E(X) = \sum_{e_{ij} \in \mathcal{C}} \nabla^{(i)} E_{\text{elast}}^{\text{cable}}(e_{ij}) + \nabla^{(i)} E_{\text{ext}}(X), \quad i = M+1, \dots, N.$$

The problem of showing the continuity of the differential can thus be reduced to proving that the equations above are continuous for all X . By (5), the last term in the equations simplifies to $(0, 0, m_i g)^T$, which we recognise as a constant in \mathbb{R}^3 , thus being infinitely differentiable. Using (3) and noting that $L(e_{ij}) = \|x^{(i)} - x^{(j)}\|$, we have that

$$\nabla^{(i)} E_{\text{elast}}^{\text{cable}}(e_{ij}) = \begin{cases} \frac{k}{\ell_{ij}^2} (L(e_{ij}) - \ell_{ij}) \cdot \frac{x^{(i)} - x^{(j)}}{L(e_{ij})} & \text{if } L(e_{ij}) > \ell_{ij}, \\ 0 & \text{if } L(e_{ij}) \leq \ell_{ij}, \end{cases} \quad (11)$$

by use of the chain rule. We observe that if $L \rightarrow \ell_{ij}^+$, then $\nabla^{(i)} E_{\text{elast}}^{\text{cable}} \rightarrow 0$, which implies that $\nabla^{(i)} E_{\text{elast}}^{\text{cable}}$ is continuous for all $e_{ij} \in \mathcal{C}$. Thus ∇E is continuous and $E \in C^1$ unconditionally, which we wanted to prove.

Unfortunately, the second derivatives of the energy function E are not necessarily continuous. We can easily show this by examining the Hessian of the energy function H_E , which we might express as

$$H_E = \nabla \otimes \nabla E = \begin{bmatrix} \nabla^{(M+1)} \nabla^{(M+1)} E & \nabla^{(M+1)} \nabla^{(M+2)} E & \dots & \nabla^{(M+1)} \nabla^{(N)} E \\ \nabla^{(M+2)} \nabla^{(M+1)} E & \nabla^{(M+2)} \nabla^{(M+2)} E & \dots & \nabla^{(M+2)} \nabla^{(N)} E \\ \vdots & \vdots & \ddots & \vdots \\ \nabla^{(N)} \nabla^{(M+1)} E & \nabla^{(N)} \nabla^{(M+2)} E & \dots & \nabla^{(N)} \nabla^{(N)} E \end{bmatrix},$$

using (10). We can then apply the product rule to (11) to get an expression for the diagonal terms of the Hessian,

$$(H_E)_{ii} = \begin{cases} \frac{k}{\ell_{ij}^2 L^2(e_{ij})} \left[\left(1 - \frac{L(e_{ij}) - \ell_{ij}}{L(e_{ij})} \right) \tilde{x} \otimes \tilde{x} + (L(e_{ij}) - \ell_{ij}) L(e_{ij}) \right] & \text{if } L(e_{ij}) > \ell_{ij}, \\ 0 & \text{if } L(e_{ij}) \leq \ell_{ij}, \end{cases}$$

where $\tilde{x} := (x^{(i)} - x^{(j)})$, $i = 1, \dots, N$. Observe that if $L \rightarrow \ell_{ij}^+$, then $(H_E)_{ii} \rightarrow \frac{k}{\ell_{ij}^4} (x^{(i)} - x^{(j)}) \otimes (x^{(i)} - x^{(j)})$, which is not necessarily equal to zero. Thus the diagonal elements of H_E might not be continuous, which implies that H_E is not continuous in general. This in turn implies that $E \notin \mathcal{C}^2$ in the general case.

Another important property in optimising the cable-net problem we want to look for is convexity.

Theorem 4 *The energy for the cable-nets (9) is convex, but not strictly convex.*

We want to determine whether the energy function in (9) is convex on its domain. We start by noting that E_{ext} is a linear function and that the second derivatives of E_{ext} all evaluate to zero. This implies that E_{ext} is convex, but not strictly convex.

Now we consider $E_{\text{elast}}^{\text{cable}}(X)$. The sum of convex functions is convex. Therefore, if each term, $E_{\text{elast}}^{\text{cable}}(e_{ij})$ is convex, then $E_{\text{elast}}^{\text{cable}}(X)$ is convex. We define a new function

$$g(K) = \begin{cases} \frac{k}{2\ell_{ij}^2} (K - \ell_{ij})^2, & K > \ell_{ij} \\ 0, & K \leq \ell_{ij} \end{cases}, \quad K \in \mathbb{R}. \quad (12)$$

Note that $g(L(e_{ij})) = E_{\text{elast}}^{\text{cable}}(e_{ij})$, where $L(e_{ij}) = \|x^{(i)} - x^{(j)}\|$ is the Euclidean norm, which is convex because the Cauchy-Schwarz theorem ensures the triangle inequality is satisfied. We find the derivative of g ,

$$g'(K) = \begin{cases} \frac{k}{\ell_{ij}^2} (K - \ell_{ij}), & K > \ell_{ij} \\ 0, & K \leq \ell_{ij} \end{cases}. \quad (13)$$

The first part of $g(K)$ is a constant, while the second part is a positive half parabola, which means that $g(K)$ is convex. $g'(K) \geq 0$, $\forall K \in \mathbb{R}$ which means that $g(K)$ is a non-decreasing function. $L : \mathbb{R}^3 \rightarrow \mathbb{R}$, $g : \mathbb{R} \rightarrow \mathbb{R}$, are both convex, and g is non-decreasing. It remains to show that if g is convex and non-decreasing and L is convex, then $g(L(x))$ is convex. By definition

$$L(\lambda x + (1 - \lambda)y) \leq \lambda L(x) + (1 - \lambda)L(y), \quad \forall x, y \in \mathbb{R}^3, \lambda \in [0, 1].$$

Inserting into g :

$$\begin{aligned} g(L(\lambda x + (1 - \lambda)y)) &\leq g(\lambda L(x) + (1 - \lambda)L(y)) \\ &\leq \lambda g(L(x)) + (1 - \lambda)g(L(y)), \quad \forall x, y \in \mathbb{R}^3, \lambda \in [0, 1]. \end{aligned}$$

The first inequality is a result of g being non-decreasing and L being convex, and the second inequality is a result of g being convex. By this, we can conclude that both E_{ext} and $E_{\text{elast}}^{\text{cable}}$ are convex, and therefore (9) is convex, but not strictly convex. This means that any local minima must necessarily also be a global minima, but not necessarily a unique global minima.

Necessary and sufficient conditions for the cable net problem (9)

The problem of minimising (9) is, as we have just proven, a convex minimisation problem where the objective function E is continuously differentiable. Thus, X^* is a global minimiser of E if and only if the gradient of E at X^* equals to zero. Furthermore, since some of the nodes in (9) are fixed, i.e. $x^{(i)} = p^{(i)}$ where $i = 1, \dots, M$, we only need to solve for the free nodes. The necessary and sufficient optimality conditions for the minimisation of (9), are therefore

$$\nabla E(X^*) = 0.$$

Tensegrity domes

Consider now the situation where we have both bars and cables in the structure as well as the constraint of fixed nodes. The optimisation problem can thus be formulated as

$$\begin{aligned} \min_X E(X) &= \sum_{e_{ij} \in \mathcal{B}} (E_{\text{elast}}^{\text{bar}}(e_{ij}) + E_{\text{grav}}^{\text{bar}}(e_{ij})) + \sum_{e_{ij} \in \mathcal{C}} E_{\text{elast}}^{\text{cable}}(e_{ij}) + E_{\text{ext}}(X) \\ \text{s.t. } x^{(i)} &= p^{(i)}, i = 1, \dots, M. \end{aligned} \quad (14)$$

Note that the problem mentioned above becomes a free optimisation problem after replacing the variables $x^{(i)}$ with the constants $p^{(i)}$, and that we now, contrary to the previous part, end up with a 3-dimensional structure.

We now want to know whether the problem posed in (14) is solvable. Therefore, we need to check for differentiability.

Theorem 5 *The function for E given by (14) is not differentiable.*

Taking the gradient of E , we get

$$\begin{aligned} \nabla E(X) &= \nabla \sum_{e_{ij} \in \mathcal{B}} (E_{\text{elast}}^{\text{bar}}(e_{ij}) + E_{\text{grav}}^{\text{bar}}(e_{ij})) + \nabla \sum_{e_{ij} \in \mathcal{C}} E_{\text{elast}}^{\text{cable}}(e_{ij}) + \nabla E_{\text{ext}}(X) = \\ &= \sum_{e_{ij} \in \mathcal{B}} (\nabla^{(i)} E_{\text{elast}}^{\text{bar}}(e_{ij}) + \nabla^{(i)} E_{\text{grav}}^{\text{bar}}(e_{ij})) + \sum_{e_{ij} \in \mathcal{C}} \nabla^{(i)} E_{\text{elast}}^{\text{cable}}(e_{ij}) + \nabla^{(i)} E_{\text{ext}}(X) \end{aligned}$$

As one might recall, we have previously shown that for structures made of cables, the energy is differentiable. In other words,

$$\sum_{e_{ij} \in \mathcal{C}} \nabla^{(i)} E_{\text{elast}}^{\text{cable}}(e_{ij}) + \nabla^{(i)} E_{\text{ext}}(X) \in C^1(\mathbb{R}^d)$$

Since the only difference between tensegrity-domes and cable structures is the addition of bars, we only have to show that either $E_{\text{elast}}^{\text{bar}}$ or $E_{\text{grav}}^{\text{bar}}$ are not differentiable. Starting by taking the gradient of $E_{\text{elast}}^{\text{bar}}$, we end up with

$$\nabla^{(i)} E_{\text{grav}}^{\text{bar}}(e_{ij}) = \left(\partial_{x_1}^{(i)} E_{\text{grav}}^{\text{bar}}, \partial_{x_2}^{(i)} E_{\text{grav}}^{\text{bar}}, \partial_{x_3}^{(i)} E_{\text{grav}}^{\text{bar}} \right)^{\top} = \left(0, 0, \frac{1}{2} \rho g l_{ij} \right),$$

which obviously is continuous for all $x \in \mathbb{R}^d$.

Lastly, the gradient for $E_{\text{bar}}^{\text{elast}}$ becomes

$$\begin{aligned} \nabla^{(i)} E_{\text{bar}}^{\text{elast}}(e_{ij}) &= \left(\partial_{x_1}^{(i)} E_{\text{bar}}^{\text{elast}}, \partial_{x_2}^{(i)} E_{\text{bar}}^{\text{elast}}, \partial_{x_3}^{(i)} E_{\text{bar}}^{\text{elast}} \right)^{\top} = \\ &= \left(\frac{c}{l_{ij}^2} (x_1^{(i)} - x_1^{(j)}) \left(1 - \frac{l_{ij}}{\|x^{(i)} - x^{(j)}\|} \right), \frac{c}{l_{ij}^2} (x_2^{(i)} - x_2^{(j)}) \left(1 - \frac{l_{ij}}{\|x^{(i)} - x^{(j)}\|} \right), \frac{c}{l_{ij}^2} (x_3^{(i)} - x_3^{(j)}) \left(1 - \frac{l_{ij}}{\|x^{(i)} - x^{(j)}\|} \right) \right)^{\top} \end{aligned}$$

As we can see, the gradient of $E_{\text{bar}}^{\text{elast}}$ is not differentiable whenever $\|x^{(i)} - x^{(j)}\| \rightarrow 0$, i.e. whenever $e_{ij} \rightarrow 0$, resulting in

$$\lim_{e_{ij} \rightarrow 0} \nabla E(X) = -\infty$$

Thus, $E(X)$ is not differentiable. This, however, does not pose a problem in practice as whenever $\|x^{(i)} - x^{(j)}\| \rightarrow 0$, the structure's bars get shorter and shorter. At some point, when $\|x^{(i)} - x^{(j)}\| = 0$, the given bar has no length, i.e. the length is zero, meaning that $E(X)$ still is differentiable as the bars that cause the lack of differentiability do not exist at all.

Theorem 6 (14) *is non-convex whenever the system has bars, that is, whenever $\mathcal{B} \neq \emptyset$.*

To keep our proof as clear and simple as possible, we will show that the full optimisation problem (14) is non-convex whenever $\mathcal{B} \neq \emptyset$ through a counter-example. To do so, recall the convexity condition given by

$$E(\lambda X + (1 - \lambda)Y) \leq \lambda E(X) + (1 - \lambda)E(Y), \quad (15)$$

where $0 \leq \lambda \leq 1$ and X, Y represent a pair of structures.

Now let X and Y be structures made of bars only such that $\mathcal{C} = \{\emptyset\}$. Moreover, let $\lambda = \frac{1}{2}$ and assume $X = -Y$, where both structures have equal length of bars such that

$$\|x^{(i)} - x^{(j)}\|_2 = \|y^{(i)} - y^{(j)}\|_2 = l_{ij}.$$

The right-hand side of (15)

$$E(\lambda X + (1 - \lambda)Y) = E\left(\frac{1}{2}X - \frac{1}{2}X\right) = E(0) = \sum_{e_{ij} \in \mathcal{B}} \frac{c}{2l_{ij}^2} (\|0 - 0\|_2 - l_{ij})^2 = \sum_{e_{ij} \in \mathcal{B}} \frac{c}{2} > 0.$$

On the other side,

$$\lambda E(X) + (1 - \lambda)E(Y) = \frac{1}{2}E(X) + \frac{1}{2}E(-X) = \frac{1}{2}E(X) - \frac{1}{2}E(-X) = 0.$$

As we can see, (15) does not hold, and hence, the minimisation problem (14) is non-convex whenever $\mathcal{B} \neq \emptyset$.

Necessary and sufficient conditions for the optimisation problem

The necessary condition for our problem is given by

$$\nabla E(X^*) = 0, \quad (16)$$

where X^* is a local solution to the optimisation problem (14). However, since E is non-convex, we also need its Hessian to be positive semi-definite so that X^* is a strict local minimised of E . As previously shown, E is not even differentiable, let alone twice differentiable. Thus, the condition (16) is not sufficient and we therefore cannot confirm whether X^* is indeed an isolated, strict local minimised of E .

Note that the non-convex nature of the optimisation problem does not necessarily mean that it does not admit local minimisers. Quite on the contrary as we will show now.

Theorem 7 *The minimisation problem given by (14) may still admit (non-global) local minimisers.*

We show this with the help of a numerical example. In figure 1, we have a system consisting of four fixed nodes and one free node, where $c, \rho g > 0$. The four fixed nodes are attached to the free nodes with bars. The global minimiser for this system is to the right, while there still exists a local minimiser to the left. Any movement in the points will increase the total energy. Thus, the minimisation problem given by (14) may still admit (non-global) local minimisers.

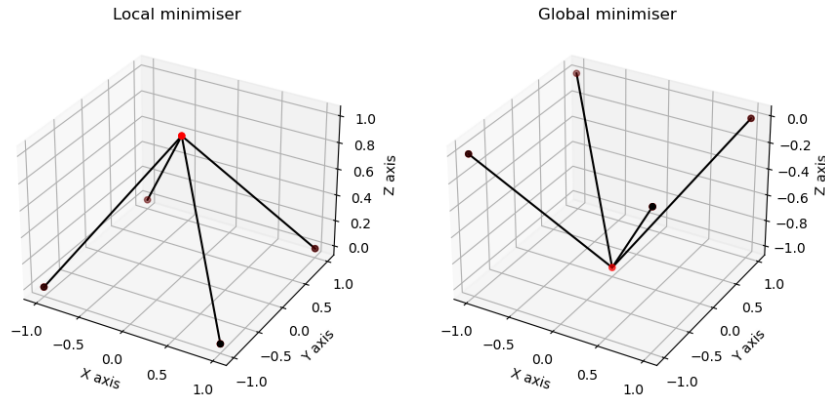


Figure 1: Local and global minimisers of the same tensegrity structure, consisting of five nodes, four of which are fixed. The black and red dots represent fixed and free nodes respectively, while the connecting line segments represent the structural bars.

Freestanding tensegrity structures

The freestanding structures have no fixed nodes, but we introduce the constraint presented in (7), where we use

$$f(x_1^{(i)}, x_2^{(i)}) = \frac{1}{20} \left((x_1^{(i)})^2 + (x_2^{(i)})^2 \right). \quad (17)$$

From the function, our constraint immediately follows as

$$c_i(X) = \begin{cases} x_3^{(i)} - f(x_1^{(i)}, x_2^{(i)}), & \text{if } x_3^{(i)} < f(x_1^{(i)}, x_2^{(i)}) \\ 0, & \text{else.} \end{cases} \quad (18)$$

$$\nabla c_i(X) = \begin{cases} \left[(0, 0, 0)_1, \dots, \left(-\frac{1}{10}x_1^{(i)}, -\frac{1}{10}x_2^{(i)}, 1 \right)_i, \dots, (0, 0, 0)_N \right]^\top, & \text{if } c_i \in \mathcal{A}(X), \\ \vec{0}, & \text{else.} \end{cases} \quad (19)$$

Note that $\nabla c_i(X)$ is a $3N$ long vector, the internal parenthesis is just for visualization. To turn the constraint optimisation problem into a free optimisation problem we use the quadratic penalty function resulting in the new objective function

$$\min_X E(X) = \sum_{e_{ij} \in \mathcal{B}} (E_{\text{elast}}^{\text{bar}}(e_{ij}) + E_{\text{grav}}^{\text{bar}}(e_{ij})) + \sum_{e_{ij} \in \mathcal{C}} E_{\text{elast}}^{\text{cable}}(e_{ij}) + E_{\text{ext}}(X) + \frac{\mu}{2} \sum_{i=1}^N c_i(X)^2, \quad (20)$$

where μ is some positive scalar. Now we can define the Lagrangian

$$\mathcal{L}(X, \lambda) = E(X) - \sum_{i=1}^N \lambda_i c_i(X). \quad (21)$$

The KKT-conditions making the first order optimality conditions now becomes

- i) $\nabla_X \mathcal{L}(X^*, \lambda^*) = 0$,
- ii) $c_i(X^*) \geq 0, \quad i = 1, \dots, N$,
- iii) $\lambda_i^* \geq 0, \quad i = 1, \dots, N$,
- iv) $\lambda_i^* c_i(X^*) = 0, \quad i = 1, \dots, N$.

Recall the definition of the constraint qualification LICQ. LICQ holds if the set of active constraints gradients $\{\nabla c_i(X), i \in \mathcal{A}(X)\}$ are linearly independent. From (19), we can see that the active gradient constraints cannot be the zero-vector. For ∇c_i the only possible non-zero entries are the indices $[3i-2, 3i-1, 3i]$. Since all the active constraint gradients have different indices for the non-zero entries, the inner product of any two active constraint gradients is zero. Thus, the active gradient vectors are linearly independent and LICQ holds.

Numerical experiments

We will now discuss the methods we have used for some different numerical experiments. We have experimented with Nelder-Mead, gradient descent and BFGS method. We decided to use the BFGS method with weak Wolfe conditions, as BFGS ensures convergence if the objective function is convex and C^2 , which is only true when solving for (9). Although the gradient descent method presents a better guarantee of convergence, we have selected BFGS since it converges faster. When introducing constraint optimisation we have applied the quadratic penalty function. One can find the code that is used in [1].

Method and functions

For the BFGS method, we use Algorithm 6.1 given in the course book [2]. When initiating the method the initial inverse Hessian approximation, H_0 , is guessed to be the identity matrix. The optimal solution is attained if we reach some maximum number of iterations or the gradient is sufficiently small. The line search method we apply, consists of two phases [1]. The first phase, the extrapolation phase, uses the Armijo and curvature conditions, eq. 3.6 in [2], to find a range for the step size that ensures a sufficient decrease in function value and adequate gradient reduction. The interpolation phase then narrows down within this range to a specific step size that strikes the right balance between making progress toward minimising the function and maintaining control over the search direction's effectiveness, satisfying both criteria. We initialise the search using $c_1 = 0.01$, $c_2 = 0.9$ and $\rho = 2$.

When minimising the energy for the freestanding structures, (20), we add (19) to our gradient term, and iteratively

increase the weight for the penalty by the following pseudo-code;

1. Initialize a structure instance
2. Set $\mu = 1$
3. $x_{\text{old}} = \text{Run BFGS algorithm with some initial coordinates}$
4. For $i = 1$ to max iterations
 - a. $\mu = \mu \cdot 5$
 - b. $x_{\text{new}} = \text{Run the BFGS algorithm from } x_{\text{old}}$
 - c. If $\|x_{\text{new}} - x_{\text{old}}\| < \text{tol}$
 - c1. Break and print the final result
 - d. $x_{\text{old}} = x_{\text{new}}$
5. Plot x_{old} .

Finally, we use the **Structure** class [1] to initialize tensegrity objects and simple cable structures. We use the class to calculate the gradient needed in the BFGS Method as well as the quadratic penalty.

Cable structure

The first case we consider is the convex, free optimisation case where our structure only consists of nodes and cables. Here we have four fixed nodes and four free nodes, and use the following parameters:

- $k = 3$, $l_{ij} = 3$ for all edges (i, j) , $m_i g = \frac{1}{6}$ for $i = 5, 6, 7, 8$.
- $p^{(1)} = (5, 5, 0)$, $p^{(2)} = (-5, 5, 0)$, $p^{(3)} = (-5, -5, 0)$, $p^{(4)} = (5, -5, 0)$.

In Figure 2 one can see the initial position, as well as the approximation for the global minimum that was found. We see that the numerical solution, shown in table 1, is the same as the analytical one.

node	1 st coordinate	2 nd coordinate	3 rd coordinate
$x^{(5)}$	2	2	-1.5
$x^{(6)}$	-2	2	-1.5
$x^{(7)}$	-2	-2	-1.5
$x^{(8)}$	2	-2	-1.5

Table 1: Optimised solution for the cable-net problem

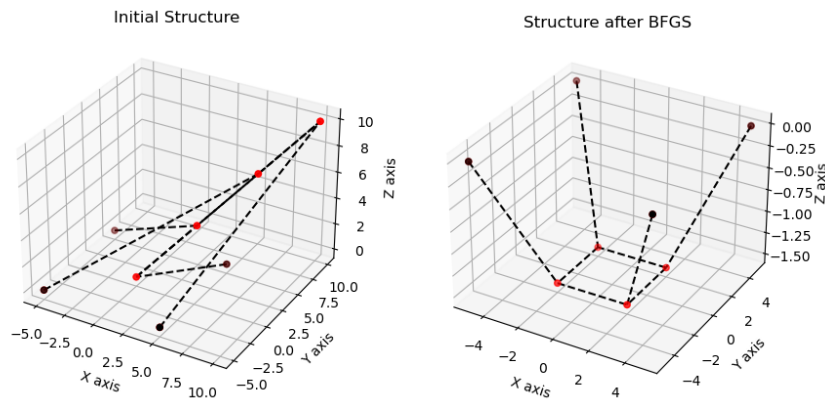


Figure 2: Initial node placement and optimised placement as computed by the BFGS method. The black and red dots represent fixed and free nodes respectively, while the dotted line segments represent the structural cables.

Tensegrity structure with fixed nodes

In the second case, we no longer have a convex optimisation problem. We introduce the bars to the tensegrity system, where we use the following parameters:

- $l_{15} = l_{26} = l_{37} = l_{48} = 10$, which is the length for the bars. $l_{18} = l_{25} = l_{36} = l_{47} = 8$ and $l_{56} = l_{67} = l_{78} = l_{58} = 1$, which are the lengths for cables.
- $c = 1$, $k = 0.1$, $\rho g = 0$, $m_i g = \frac{1}{6}$ for $i = 5, 6, 7, 8$.
- $p^{(1)} = (1, 1, 0)$, $p^{(2)} = (-1, 1, 0)$, $p^{(3)} = (-1, -1, 0)$, $p^{(4)} = (1, -1, 0)$.

In figure 3, one can see the initial position and the local minimum found by the numerical method. We see that we find the desired analytical solution with an error of 10^{-8} for all free variables. This is due to the tolerance we decide for the numerical method. Note that in practice the lack of smoothness will not matter due to the discontinuities only applying when the bars have zero length. The optimal placement of the free nodes, as computed by the BFGS algorithm, are listed in table 2.

node	1 st coordinate	2 nd coordinate	3 rd coordinate
$x^{(5)}$	$-7.09710266 \cdot 10^{-1}$	$-1.27678494 \cdot 10^{-8}$	9.54287110
$x^{(6)}$	$1.89984151 \cdot 10^{-8}$	$-7.09710304 \cdot 10^{-1}$	9.54287109
$x^{(7)}$	$7.09710309 \cdot 10^{-1}$	$-1.90081917 \cdot 10^{-8}$	9.54287110
$x^{(8)}$	$2.56812428 \cdot 10^{-8}$	$7.09710272 \cdot 10^{-1}$	9.54287111

Table 2: Optimised solution for the tensegrity dome.

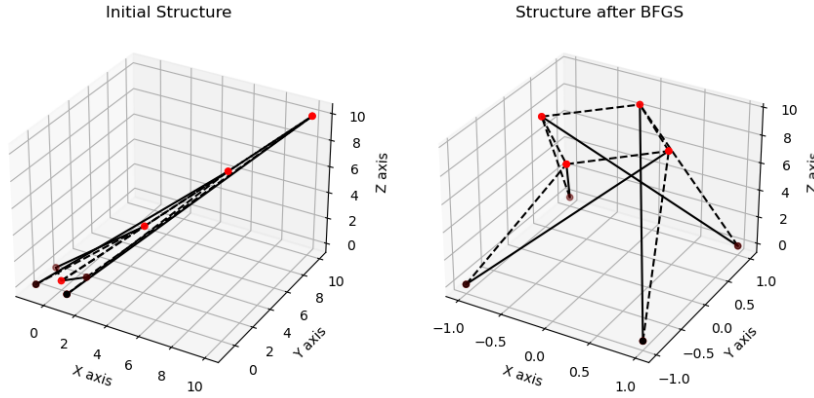


Figure 3: Initial node placement and optimised placement as computed by the BFGS method. The black and red dots represent fixed and free nodes respectively, while the line segments represent the structural members. Dotted line segments correspond to structural cables and solid line segments correspond to structural bars.

Freestanding tensegrity structures

For the final and most interesting scenario, we consider the free-standing tensegrity structures. The first structure is almost the same as the previous structure. However, all nodes are now free and we introduce/change the following variables:

- $l_{12} = l_{23} = l_{34} = l_{14} = 2$, which are the length for the cables.
- $\rho g = 10^{-4}$.
- $f(x_1, x_2) = \frac{(x_1^2 + x_2^2)}{20}$ for the ground level.

In Figure 4, one can see the initial position and the final solution for the local minimum we found. For the first two problems, the numerical method needed almost no guidance for convergence to the desired solution. However, for this problem and the next and final structure, many initial positions do not converge to the desired/interesting solutions. For the final free-standing structure, we try to add another four free nodes on top of the previous system. We introduce the new cables and bars:

- $l_{5,9} = l_{6,10} = l_{7,11} = l_{8,12} = 10$, which is the length for the bars. $l_{5,10} = l_{6,11} = l_{7,12} = l_{8,9} = 8$ and $l_{9,10} = l_{10,11} = l_{11,12} = l_{9,12} = 2$, which is the length for the cables.

Given some reasonable initialization nodes, we can see from figure 5 that the method succeeds in finding a free-standing local solution, where the four new nodes are stacked on top of the previous structure.

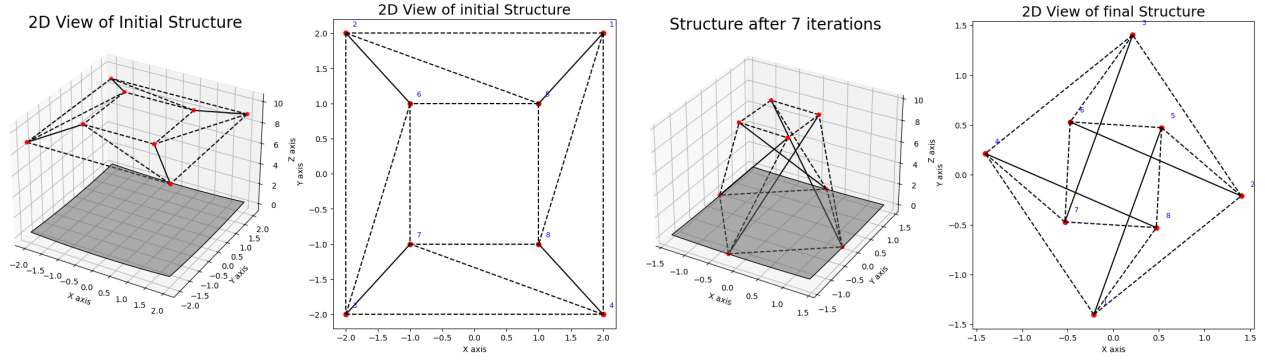


Figure 4: Initial node placement and optimised placement after 7 iterations of the BFGS algorithm with a quadratic penalty term accounting for the ground profile, both of which are available as a three-dimensional plot and as a projection onto the ground profile. The red dots represent free nodes, while the line segments represent the structural members. Dotted line segments correspond to structural cables and solid line segments correspond to structural bars. The ground profile are shown in grey in the three-dimensional plots.

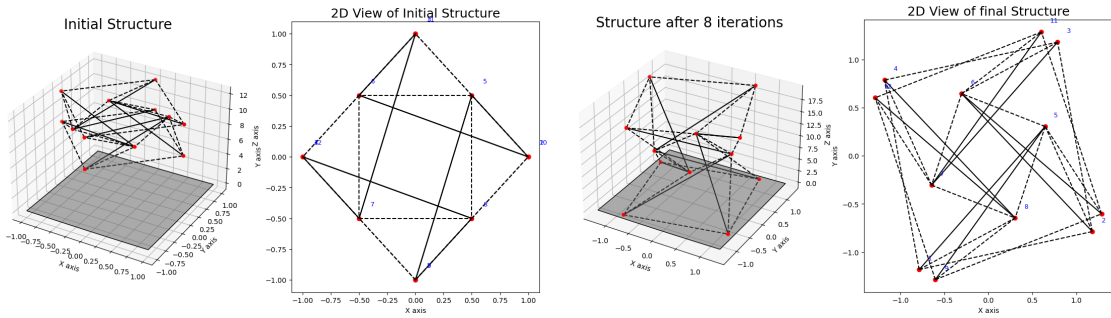


Figure 5: Initial node placement and optimised placement after 8 iterations of the BFGS algorithm with a quadratic penalty term accounting for the ground profile, both of which are available as a three-dimensional plot and as a projection onto the ground profile. The red dots represent free nodes, while the line segments represent the structural members. Dotted line segments correspond to structural cables and solid line segments correspond to structural bars. The ground profile are shown in grey in the three-dimensional plots.

Conclusion

We know from simple mechanics, that a stable tensegrity structure is obtained whenever the structure's energy is at a minimum. Using theory of optimisation, it is possible to formulate necessary, and in some cases sufficient, optimality conditions for the energy corresponding to the shapes of such structures. We are thus able to compute valid shapes of tensegrity structures, by finding shapes that satisfy the above mentioned conditions. This can be done numerically, e.g. by use of the BFGS method, adding a quadratic penalty term to account for the ground profile in cases where the structure is freestanding. Although the problem of determining the shape of tensegrity domes and freestanding tensegrity structures only omit sufficient optimality conditions, due to the non-convex nature of the underlying problems, the BFGS method provides valid solutions to the problems in question.

References

- [1] *Optimisation-Project*. <https://github.com/Taape2071/Optimisation-Project.git>. 2024.
- [2] J. Nocedal and S. J. Wright. *Numerical Optimization*. Springer New York, NY, 2006.
- [3] OpenAI. *ChatGPT*. Version stable release, 13. February. 2024. URL: <https://chat.openai.com/>. Remark: Has been used sparingly as an aid in the creation of the following python functions, `H_update()`, `plot_3D_points()`, `plot_3D_points_2()` and `line_search_wolfe()`. All these functions are found in [1].